Numerical Heat Transfer, Part A: Applications: An International Journal of Computation and Methodology
Publication details, including instructions for authors and subscription information:
http://www.tandfonline.com/loi/unht20

Numerical Investigation of Heat Transfer from a Heated Oscillating Rectangular Cylinder in a Cross Flow

Suh-Jenq Yang, Wu-Shung Fu
Published online: 29 Oct 2010.

To cite this article: Suh-Jenq Yang, Wu-Shung Fu (2001) Numerical Investigation of Heat Transfer from a Heated Oscillating Rectangular Cylinder in a Cross Flow, Numerical Heat Transfer, Part A: Applications: An International Journal of Computation and Methodology, 39:6, 569-591, DOI: 10.1080/10407780121190

To link to this article: http://dx.doi.org/10.1080/10407780121190

Numerical Heat Transfer, Part A, 39:569–591, 2001

1040-7782/01 $12.00 + .00

NUMERICAL INVESTIGATION OF HEAT TRANSFER FROM A HEATED OSCILLATING RECTANGULAR CYLINDER IN A CROSS FLOW

Suh-Jenq Yang
Department of Industrial Engineering and Management, Nan Kai Institute of Technology, Nantou, 542, Taiwan, Republic of China

Wu-Shung Fu
Department of Mechanical Engineering, National Chiao Tung University, Hsinchu, 30056, Taiwan, Republic of China

A numerical simulation is performed to study the flow structures and heat transfer characteristics of a heated transversely oscillating rectangular cylinder in a cross flow. The variations of flow and thermal fields are classified into a class of the moving boundary problems. The moving interfaces between the fluid and rectangular cylinder have been considered. An arbitrary Lagrangian–Eulerian (ALE) kinematic description method is adopted to describe the flow and thermal fields. A penalty consistent finite element formulation is applied to solve the governing equations. The subsequent developments of the vortex shedding and heat transfer characteristics around the heated rectangular cylinder are presented in detail. The effects of Reynolds number, oscillating amplitude, oscillating speed, blockage ratio, and aspect ratio on the flow structures and heat transfer characteristics are examined. The results show that the interaction between the oscillating rectangular cylinder and vortex shedding from the rectangular cylinder dominates the state of the wake. The flow and thermal fields may approach a periodic state with time. The heat transfer around the rectangular cylinder performance is enhanced remarkably.

INTRODUCTION

A phenomenon of vortex shedding induced by a flow passing through a stationary or an oscillating circular cylinder is frequently encountered in engineering applications, such as a hot-wire anemometer, heat exchanger tube, and nuclear reactor fuel rod. Doubtless, the heat transfer mechanism of the circular cylinder in the flow of vortex shedding is also interesting and important in the above engineering applications. Several researchers have investigated the flow structures and heat transfer characteristics of the above subject.

Received 11 September 2000; accepted 1 November 2000.

The support ofthis work by the National Science Council of Taiwan, R.O.C., under contract NSC89-2212-E-009-08 7 is gratefuly acknlowledged.

Address correspondence to Wu-Shung Fu, Department of Mechanical Engineering, National Chiao Tung University, 1001 Ta Hsueh Road, Hsinchun, Taiwan 30056, Repubic of China. E-mail: wsfu@cc.nctu.edu.tw

NOMENCLATURE

A	aspect ratio ($A = w_2/h_2$)
B	blockage ratio ($B = h_2/h$)
f	vortex shedding frequency [s^{-1}]
f_c	oscillating frequency of the rectangular cylinder [s^{-1}]
F_c	dimensionless oscillating frequency of the rectangular cylinder ($F_c = f_c h_2/u_o$)
h	dimensional height of the channel [m]
H	dimensionless height of the channel ($H = h/h_2$)
L_c	dimensionless oscillating amplitude of the rectangular cylinder ($L_c = \iota_c/h_2$)
Nu	overall Nusselt number around the rectangular cylinder
Nu_x	local Nusselt number on the top and bottom surfaces of the rectangular cylinder
$\overline{\mathrm{Nu}_Y}$	average Nusselt number on the top and bottom surfaces of the rectangular cylinder
Nu_Y	local Nusselt number on the front and rear surfaces of the rectangular cylinder
$\overline{\mathrm{Nu}_Y}$	average Nusselt number on the front and rear surfaces of the rectangular cylinder
p	dimensional pressure [$N \cdot m^{-2}$]
p_∞	referential pressure [$N \cdot m^{-2}$]
P	dimensionless pressure ($P = (p - p_\infty)/\rho u_0^2$)
Pr	Prandtl number ($\mathrm{Pr} = \nu/\alpha$)
Re	Reynolds number ($\mathrm{Re} = u_0 h_2/\nu$)
s_c	dimensional oscillating speed of the rectangular cylinder [$s \cdot s^{-1}$]
S_c	dimensionless oscillating speed of the rectangular cylinder ($S_c = s_c/u_0$)
St	Strouhal number or dimensionless vortex shedding frequency ($\mathrm{St} = f h_2/u_0$)
t	dimensional time [s]
T	dimensional temperature [°C]
T_c	dimensional temperature of the rectangular cylinder [°C]
T_0	dimensional temperature of the inlet fluids [°C]
u, v	dimensional velocities in x and y directions [$m \cdot s^{-1}$
U, V	dimensionless velocities in X and Y directions ($U = u/u_0$, $V = v/u/u_0$)
u_0	dimensional velocity of the inlet fluid [$m \cdot s^{-1}$]
v_c	dimensional oscillating velocity of the rectangular cylinder [$m \cdot s^{-1}$]
V_c	dimensionless oscillating velocity of the rectangular cylinder ($V_c = v_c/u_0$)
$\hat{v}$	dimensional mesh velocity in y-direction [$m \cdot s^{-1}$]
$\hat{V}$	dimensionless mesh velocity in Y direction ($\hat{V} = \hat{v}/u_0$)
w	dimensional length of the channel [m]
W	dimensionless length of the channel ($W = w/h_2$)
w_1	dimensional length from the inlet to the rectangular cylinder [m]
W_1	dimensionless length from the inlet to the rectangular cylinder ($W_1 = w_1/h_2$)
w_2	dimensional width of the rectangular cylinder [m]
W_2	dimensionless width of the rectangular cylinder ($W_2 = w_2/h_2$)
w_3	dimensional length from the rectangular cylinder to the outlet [m]
W_3	dimensionless length from the rectangular cylinder to the outlet ($W_3 = w_3/h_2$)
x, y	dimensional Cartesian coordinates [m]
X, Y	dimensionless Cartesian coordinates ($X = x/h_2$, $Y = y/h_2$)
$\|$	absolute value
ι_c	dimensional oscillating amplitude of the rectangular cylinder [m]
α	thermal diffusivity [$m^2 \cdot s^{-1}$]
ϕ	computational variables
λ	penalty parameter
ν	kinematic viscosity [$m^2 \cdot s^{-1}$]
θ	dimensionless temperature ($\theta = (T - T_0)/(T_c - T_0)$)
ρ	density [$kg \cdot m^{-3}$]
τ	dimensionless time ($\tau = t u_0/h_2$)
τ_p	dimensionless time of one oscillating cycle
Ψ	dimensionless stream function

For a flow passing through a stationary circular cylinder [1–4], the Strouhal number of vortex shedding was about 0.2 over a range of Reynolds numbers varying from 2×10^2 to 10^4. The unsteady flow of vortex shedding from the circular cylinder caused the heat transfer on the circular cylinder to be unsteady, and the maximum local heat transfer rate was found near the front stagnation point.

For a flow passing through an oscillating circular cylinder, Sreenivasan and Ramachandran [5] studied the effect of vibration on the heat transfer of a horizontal cylinder normal to air stream by an experimental method. The results showed that no appreciable change in the heat transfer coefficient was observed. Saxena and Laird [6], Leung et al. [7], Karanth et al. [8], and Gau et al. [9] investigated the flow structure and heat transfer around a heated oscillating circular cylinder. The results found that the enhancement of heat transfer was proportional to the magnitude of oscillating frequency and amplitude of the circular cylinder. Cheng et al. [10, 11] adopted numerical and experimental methods to study the effect of transverse oscillation on the flow patterns and heat transfer from a circular cylinder. The results indicated that the heat transfer was increased remarkably as the flow approached the lock-in regime, which occurs when the circular cylinder oscillating frequency is near the natural vortex shedding frequency; however, outside the lock-in regime the heat transfer was almost unaffected by the oscillation of the circular cylinder. Patnaik and colleagues [12] adopted a Galerkin weighted residual formulation to simulate a flow passing over an isolated circular cylinder. The effects of aiding and opposing buoyancy forces on the flow and thermal fields had been studied, and the mechanisms of vortex shedding were investigated in detail.

Instead of the circular cylinder mentioned above, a rectangular cylinder, such as building, bridge, heat exchangers, fins, and electronic components, also is a typical structure used in the investigation of vortex shedding for engineering and industrial applications. Some numerical and experimental studies [13–17] paid attention to this subject and focused on the unsteady flow of vortex shedding and the heat transfer of a stationary rectangular cylinder. The results indicated that the aspect ratio and attack angle of the rectangular cylinder were the major factors to affect the flow and thermal fields. The heat transfer of the stationary rectangular cylinder may be enhanced due to the vortex shedding.

However, most studies mentioned above focused on stationary circular and rectangular cylinders and an oscillating circular cylinder with a small oscillating amplitude. The flow of vortex shedding and the heat transfer of a rectangular cylinder affected by an oscillating rectangular cylinder with a relatively large oscillating amplitude and speed and blockage is seldom investigated. These could be applied in the fluid machinery, moving machine, heat transfer promoter, active eddy promoter, and so on.

The object of this work, therefore, is to investigate the variations of unsteady flow and thermal fields as a flow passes over a heated transversely oscillating rectangular cylinder. Because of the interaction between the flow and oscillating rectangular cylinder, the variations of the flow and thermal fields become time dependent and belong to a class of the moving boundary problems. In the past, a structure oscillating or moving in a flowing fluid was conveniently regarded as a stationary one in the flow, or a noninertial reference frame moving with the structure was considered to analyze the above problem. However, because of the con-

tinuity of flow, the fluid near the structure will simultaneously replenish the vacant space induced by the movement of the structures. For simulating the problem more realistically, the interfaces between the fluid and rectangular cylinder under a moving situation have been taken into consideration, and this problem has hardly been analyzed solely by either the Lagrangian or Eulerian kinematic description method. An ALE kinematic description method [18], which combines the characteristics of the Lagrangian and Eulerian kinematic description methods, is an appropriate kinematic description method to describe this problem. In the ALE method, the computational meshes may move with the fluid (Lagrangian), be held fixed (Eulerian), or be moved in a prescribed way. The detail of the kinematic theory of the ALE method is delineated in Hughes et al. [19], Donea et al. [20], Ramaswamy and Kwahara [21], and Ramaswamy [22].

Consequently, the ALE method is used to analyze the variations of the flow and thermal fields induced by the heated transversely oscillating rectangular cylinder in a cross flow. A consistent penalty finite element method is applied to solve the governing equations. The subsequent developments of the vortex shedding and the heat transfer characteristics around the heated rectangular cylinder are presented in detail. The effects of Reynolds number, blockage ratio, aspect ratio, oscillating speed, and oscillating amplitude of the rectangular cylinder on the flow structures and heat transfer characteristics are investigated.

PHYSICAL MODEL

A two-dimensional channel with height h and length w as shown in Figure 1 is used. A heated rectangular cylinder with width w_2 and height h_2 is set within this channel. The distances from the inlet and outlet of the channel to the rectangular cylinder are w_1 and w_3, respectively. The inlet velocity u_0 and temperature T_0 of the fluid are uniform. The heated rectangular cylinder is maintained at a constant temperature T_c, which is higher than T_0. Initially ($t = 0$), the rectangular cylinder

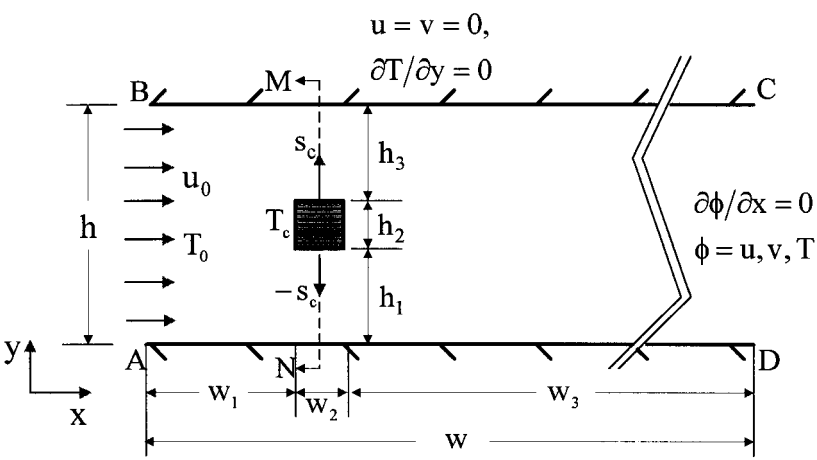

Figure 1. Physical model.

is stationary at the position of the center of the channel and the fluid flows steadily. As the time $t > 0$, the rectangular cylinder is in oscillating motion normal to the inlet flow with a constant oscillating speed s_c. Because of the interaction between the flow and oscillating rectangular cylinder, the variations of the flow and thermal fields become time dependent and the situation could be catalogued as a class of the moving boundary problems. As a result, the ALE method is properly utilized to analyze this problem.

For facilitating the analysis, the following assumptions are made.

(1) The fluid is air and the flow field is two-dimensional, incompressible, and laminar.
(2) The fluid properties are constant and the effect of the gravity is neglected.
(3) The no-slip condition is held on the interfaces between the fluid and rectangular cylinder.

Based upon the characteristic scales of h_2, u_0, ρu_0^2, and T_0, the dimensionless variables are defined as follows:

$$X = \frac{x}{h_2} \quad Y = \frac{y}{h_2} \quad U = \frac{u}{u_0} \quad V = \frac{v}{u_0}$$
$$\hat{V} = \frac{\hat{v}}{u_0} \quad V_c = \frac{v_c}{u_0} \quad S_c = \frac{s_c}{u_0} \quad P = \frac{p - p_\infty}{\rho u_0^2}$$
$$\tau = \frac{t u_0}{h_2} \quad \theta = \frac{T - T_0}{T_c - T_0} \quad \mathrm{Re} = \frac{u_0 h_2}{\nu} \quad \mathrm{Pr} = \frac{\nu}{\alpha} \tag{1}$$

where $\hat{v}$ is the mesh velocity, and v_c and $s_c\,(= |v_c|)$ are the oscillating velocity and speed of the rectangular cylinder, respectively.

According to the above assumptions and dimensionless variables, the dimensionless ALE governing equations [20–25] are expressed as the following equations:

Continuity

$$\frac{\partial U}{\partial X} + \frac{\partial V}{\partial Y} = 0 \tag{2}$$

Momentum

$$\frac{\partial U}{\partial \tau} + U\frac{\partial U}{\partial X} + (V - \hat{V})\frac{\partial U}{\partial Y} = -\frac{\partial P}{\partial X} + \frac{1}{\mathrm{Re}}\left(\frac{\partial^2 U}{\partial X^2} + \frac{\partial^2 U}{\partial Y^2}\right) \tag{3}$$

$$\frac{\partial V}{\partial \tau} + U\frac{\partial V}{\partial X} + (V - \hat{V})\frac{\partial V}{\partial Y} = -\frac{\partial P}{\partial Y} + \frac{1}{\mathrm{Re}}\left(\frac{\partial^2 V}{\partial X^2} + \frac{\partial^2 V}{\partial Y^2}\right) \tag{4}$$

Energy

$$\frac{\partial \theta}{\partial \tau} + U\frac{\partial \theta}{\partial X} + (V - \hat{V})\frac{\partial \theta}{\partial Y} = \frac{1}{\mathrm{Re\,Pr}}\left(\frac{\partial^2 \theta}{\partial X^2} + \frac{\partial^2 \theta}{\partial Y^2}\right) \tag{5}$$

As the time $\tau > 0$, the boundary conditions are as follows:

On the inlet surface AB

$$U = 1 \quad V = 0 \quad \theta = 0 \tag{6}$$

On the walls BC and AD

$$U = V = 0 \qquad \partial\theta/\partial Y = 0 \tag{7}$$

On the outlet surface CD

$$\partial U/\partial X = \partial V/\partial X = \partial\theta/\partial X = 0 \tag{8}$$

On the interfaces between the fluid and rectangular cylinder

$$U = 0 \quad V = V_c \quad \theta = 1 \tag{9}$$

NUMERICAL FORMULATION

The governing equations are solved through the consistent penalty finite element method. An implicit scheme is adopted to deal with the time terms of the governing equations. The pressure is eliminated from the momentum equations using the consistent penalty model [26]. The velocity and temperature are approximated by quadrilateral elements and a nine-node quadratic Lagrangian interpolation function. The nonlinear terms in the momentum equations are simplified by a Newton–Raphson iteration algorithm. The discretization processes of the governing equations are similar to the one used in Fu et al. [27]. The details of the numerical method and solution procedures are delineated in Fu and Yang [23–25].

The mesh velocity $\hat{V}$ is linearly distributed and inversely proportional to the distance between the nodes of the computational elements and rectangular cylinder. The relative errors of each variable to examine the convergence of solutions are defined as follows:

$$\left|\frac{\phi^{m+1} - \phi^m}{\phi^{m+1}}\right|_{\tau+\Delta\tau} < 1.0 \times 10^{-3} \quad \text{where } \phi = U, V, \theta \tag{10}$$

Besides, the conservative residual of the continuity equation

$$\text{Residual} = \frac{\partial U}{\partial X} + \frac{\partial V}{\partial Y} \tag{11}$$

is used to check for each element at each time and to ensure that the mass conservative law is satisfied. In the computing process of this study, the residual of the continuity equation for each element is smaller than 5.0×10^{-7}. The numerical computations for the governing equations are carried out until quasi-periodic solutions are obtained.

RESULTS AND DISCUSSION

The working fluid is air with $\text{Pr} = 0.71$. The main parameters of Reynolds number Re, oscillating speed S_c, oscillating amplitude $L_c\,(= \iota_c/h_2)$, blockage ratio $B\,(= h_2/h)$, and aspect ratio $A\,(= w_2/h_2)$ are examined and the combinations of these parameters are tabulated in Table 1.

Table 1. Computed parameter combinations

	Re	S_c	L_c	τ_p	F_c	B	A
Case 1	250	0.333	0.5	6.0	0.167	0.1	1.0
Case 2	500	0.333	0.5	6.0	0.167	0.1	1.0
Case 3	250	0.5	0.125	1.0	1.0	0.1	1.0
Case 4	250	0.5	0.25	2.0	0.5	0.1	1.0
Case 5	250	0.5	0.5	4.0	0.25	0.1	1.0
Case 6	250	0.5	0.75	6.0	0.167	0.1	1.0
Case 7	500	0.5	0.5	4.0	0.25	0.1	1.0
Case 8	500	1.0	0.5	2.0	0.5	0.1	1.0
Case 9	500	0.5	0.333	6.0	0.167	0.2	1.0
Case 10	500	0.5	0.333	6.0	0.167	0.1	2.0

The dimensionless oscillation frequency of the rectangular cylinder F_c and Strouhal number St (dimensionless vortex shedding frequency) are defined as $F_c = f_c h_2/u_0$ and $\mathrm{St} = f h_2/u_0$, respectively, where f_c and f are the oscillation frequency of the rectangular cylinder and vortex shedding frequency, respectively.

The local Nusselt number Nu_X and average Nusselt number $\overline{\mathrm{Nu}_X}$ on the top and bottom surfaces of the rectangular cylinder are defined as follows, respectively:

$$\mathrm{Nu}_X(X,\tau) = -\frac{\partial\theta}{\partial Y} \tag{12}$$

$$\overline{\mathrm{Nu}_X}(\tau) = \frac{1}{W_2}\int_0^{W_2} \mathrm{Nu}_X\, dX \tag{13}$$

Similarly, the local Nusselt number Nu_Y and average Nusselt number $\overline{\mathrm{Nu}_Y}$ on the front and rear surfaces of the rectangular cylinder are defined as follows, respectively:

$$\mathrm{Nu}_Y(Y,\tau) = -\frac{\partial\theta}{\partial X} \tag{14}$$

$$\overline{\mathrm{Nu}_Y}(\tau) = \frac{1}{H_2}\int_0^{H_2} \mathrm{Nu}_Y\, dY \tag{15}$$

The overall Nusselt number Nu around the rectangular cylinder is defined as

$$\mathrm{Nu}(\tau) = \frac{1}{2W_2 + 2H_2}\left(\int_0^{W_2} \mathrm{Nu}_X\big|_{\mathrm{top}}\, dX + \int_0^{W_2} \mathrm{Nu}_X\big|_{\mathrm{bottom}}\, dX + \int_0^{H_2} \mathrm{Nu}_Y\big|_{\mathrm{front}}\, dY + \int_0^{H_2} \mathrm{Nu}_Y\big|_{\mathrm{rear}}\, dY\right) \tag{16}$$

Mesh and Time Step Tests

For matching the boundary conditions at the inlet and outlet of the channel mentioned above, the lengths from the inlet and outlet to the rectangular cylinder are determined by numerical tests and are equal to 8.0 and 26.0, respectively.

To obtain an optimal computational mesh, three different nonuniform distributed elements, which provide a finer element resolution near the rectangular cylinder and walls, are used for the mesh tests. Figure 2 shows the velocity and temperature profiles along the line $\overline{MN}$ as indicated in Figure 1 at the steady state under $\mathrm{Re} = 500$, $B = 0.1$, and $A = 1.0$. Based upon the results, the computational mesh with 3,672 elements, which corresponds to 15,016 nodes, is used for all cases.

In addition, an implicit scheme is employed to deal with the time differential terms of the governing equations. Three different time steps $\Delta\tau = 0.05$, 0.01, and at $\mathrm{Re} = 500$, $S_c = 0.5$, $L_c = 0.5$, $\tau_p = 4.0$, $F_c = 0.25$, $B = 0.1$, $A = 1.0$ and are executed for the time step tests. The variations of the overall Nusselt number Nu around the rectangular cylinder with time are shown in Figure 3, and the smallest time step $\Delta\tau = 0.005$ is chosen for all cases in this study.

The dimensionless stream function Ψ is defined as

$$U = \frac{\partial \Psi}{\partial Y} \quad \text{and} \quad V = -\frac{\partial \Psi}{\partial X} \tag{17}$$

For clearly indicating the variations of the flow and thermal fields, only the streamlines and isothermal lines in the vicinity of the rectangular cylinder are presented. Besides, the arrow in the subsequent figures indicates the moving direction of the rectangular cylinder.

Effects of the Oscillating Rectangular Cylinder on the Flow and Thermal Fields

Figure 4 shows the velocity vectors of the overall computational domain and the isothermal lines around the rectangular cylinder at the steady state ($\tau = 0$) under $\mathrm{Re} = 250$, $B = 0.1$, and $A = 1.0$. The rectangular cylinder is stationary and the flow is steady. The flow separates from the leading edges of the rectangular cylinder and large recirculation zones are observed behind the rectangular cylinder. The distributions of the isothermal lines are denser near the front surface of the rectangular cylinder than those of the other surfaces of the rectangular cylinder. The overall Nusselt number Nu around the rectangular cylinder is about 5.44.

Figure 5 shows the transient development of the streamlines for case 1 ($\mathrm{Re} = 250$, $S_c = 0.333$, $L_c = 0.5$, $\tau_p = 6.0$, $F_c = 0.167$, $B = 0.1$, and $A = 1.0$). As the time $\tau > 0$, the rectangular cylinder starts to oscillate with a constant oscillating speed $S_c = 0.333$ and oscillating amplitude $L_c = 0.5$. At first, as shown in Figure 5*a*, the rectangular cylinder moves upward. The fluid near the top surface of the rectangular cylinder is pressed by the top surface of the rectangular cylinder. Conversely, the fluid near the bottom surface of the rectangular cylinder simultaneously replenishes the vacant space induced by the movement of the rectangular cylinder because of the continuity of the flow. As a result, a new recirculation zone is formed around the bottom surface of the rectangular cylinder. Afterward, the rectangular cylinder moves upward continuously until the amplitude L_c is equal to 0.5. The new recirculation zone around the bottom surface of the rectangular cylinder enlarges gradually and pushes the original large recirculation zones behind the rectangular cylinder, as shown in Figure 5*b*.

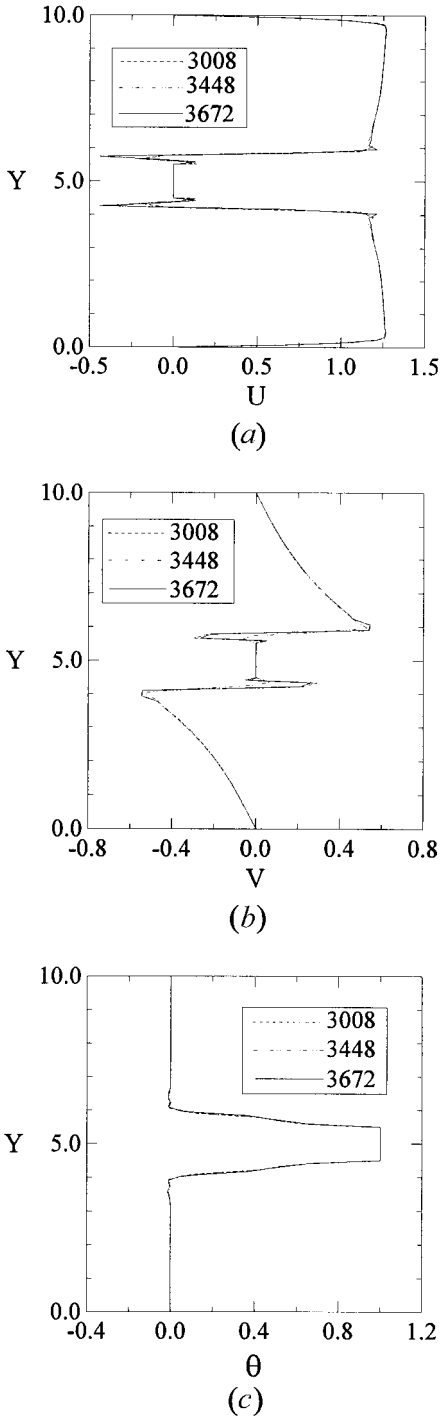

Figure 2. Comparison of the velocity and temperature profiles along the lines $\overline{MN}$ at the steady state under $\mathrm{Re} = 500$, $B = 0.1$, and $A = 1.0$ situations for various computatonal elements.

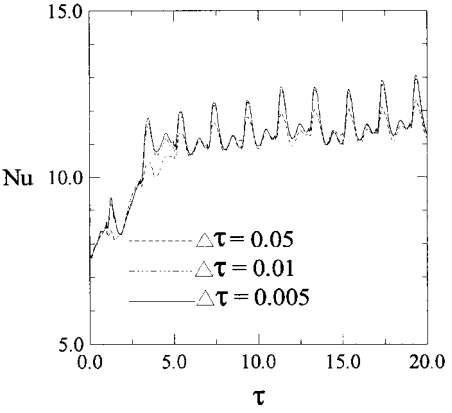

Figure 3. Comparison of the variations of the overall Nusselt number around the rectangular cylinder with time for different time steps $\Delta\tau$ under $\mathrm{Re} = 500$, $S_c = 0.5$, $L_c = 0.5$, $\tau_p = 4.0$, $F_c = 0.25$, $B = 0.1$, and $A = 1.0$ situations.

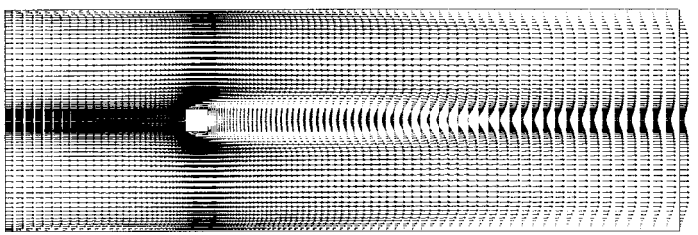

(*a*)

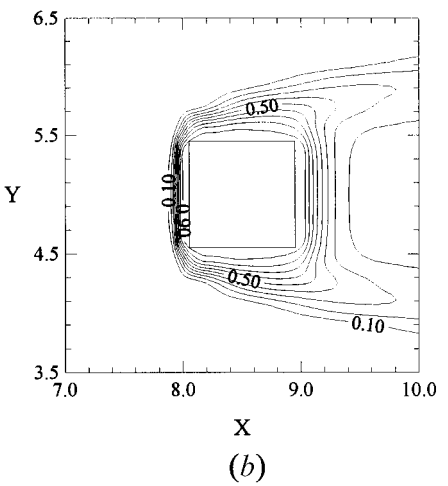

(*b*)

Figure 4. The flow and thermal fields at steady state under $\mathrm{Re} = 250$, $B = 0.1$, $A = 1.0$ situations. (*a*) Velocity vectors of overall computational domain, (*b*) isothermal lines distribution around the rectangular cylinder.

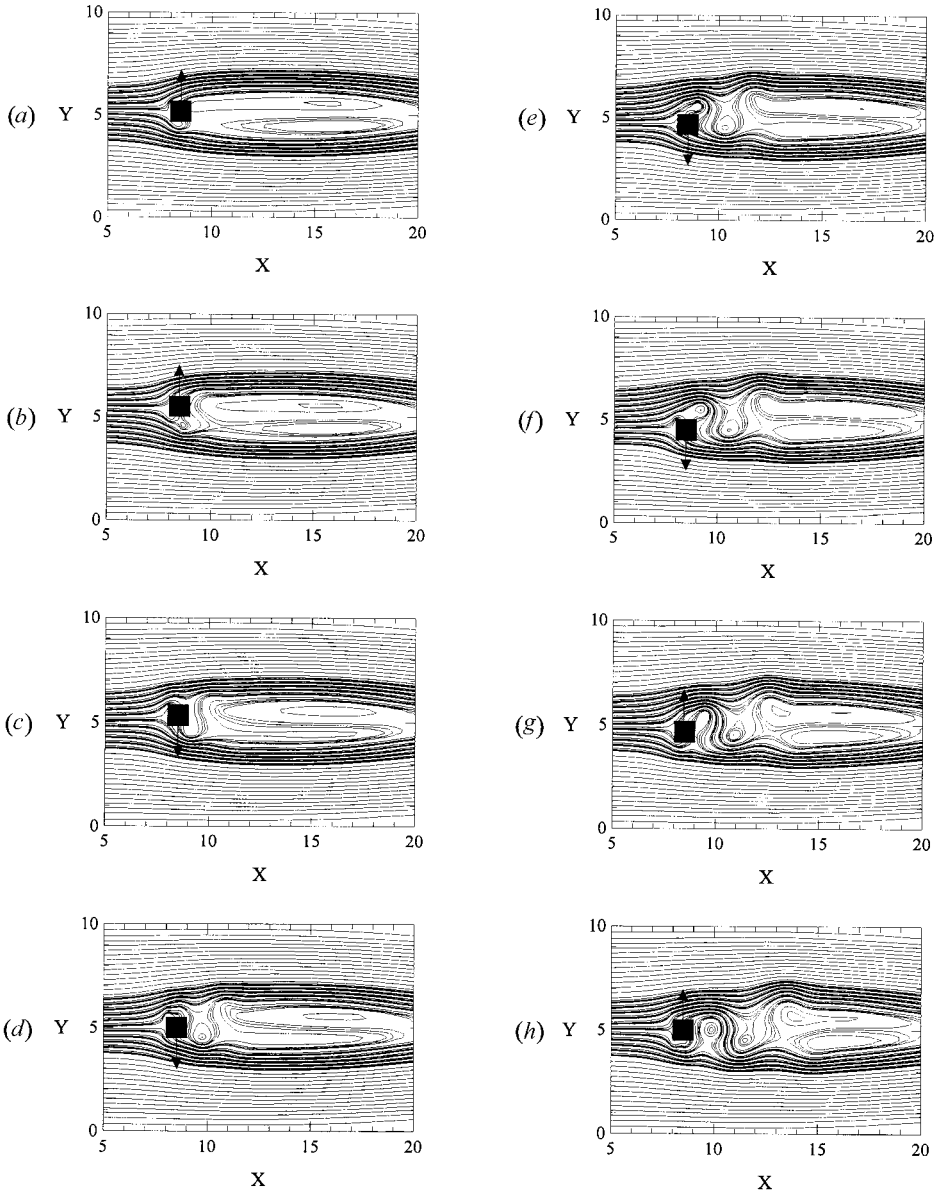

FIGURE 5

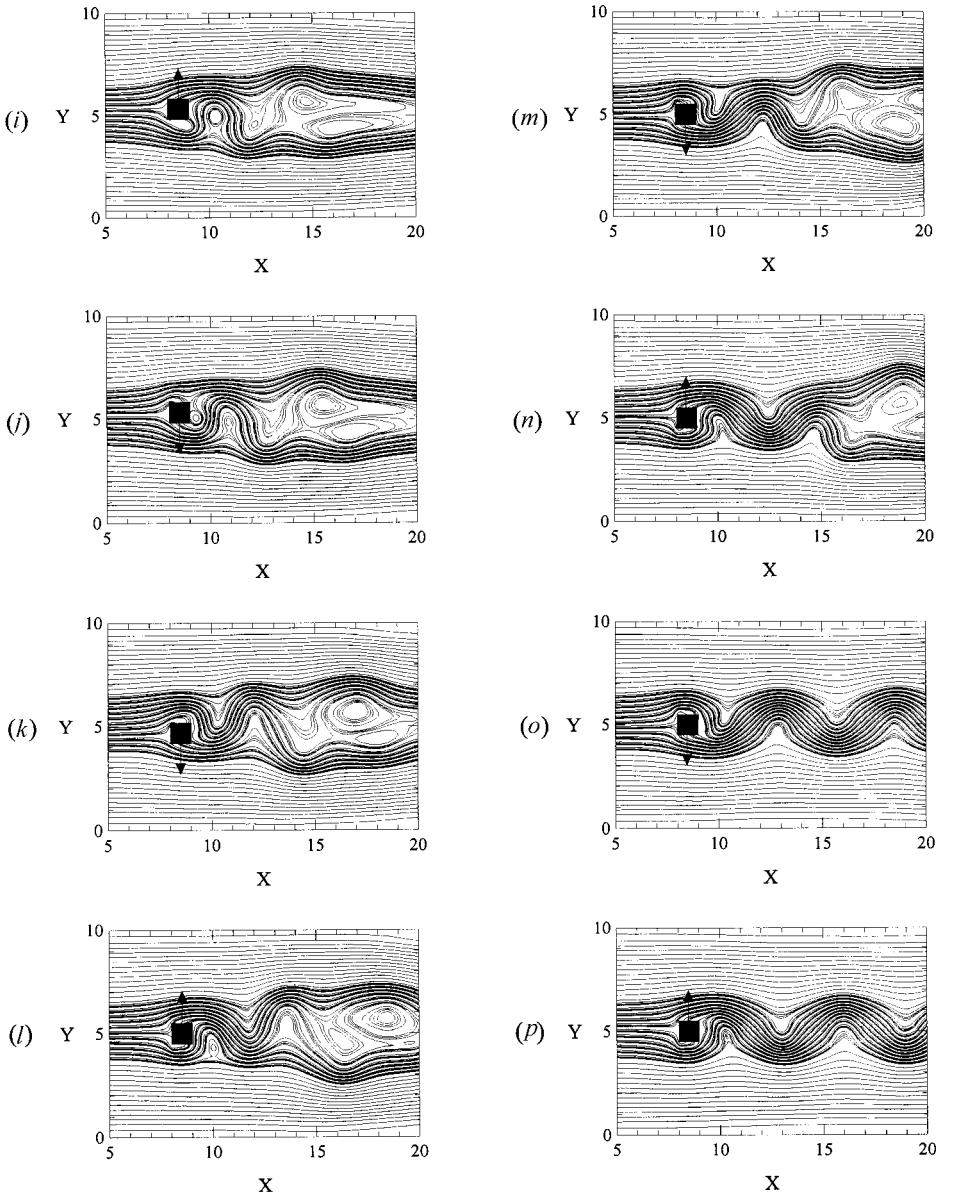

FIGURE 5

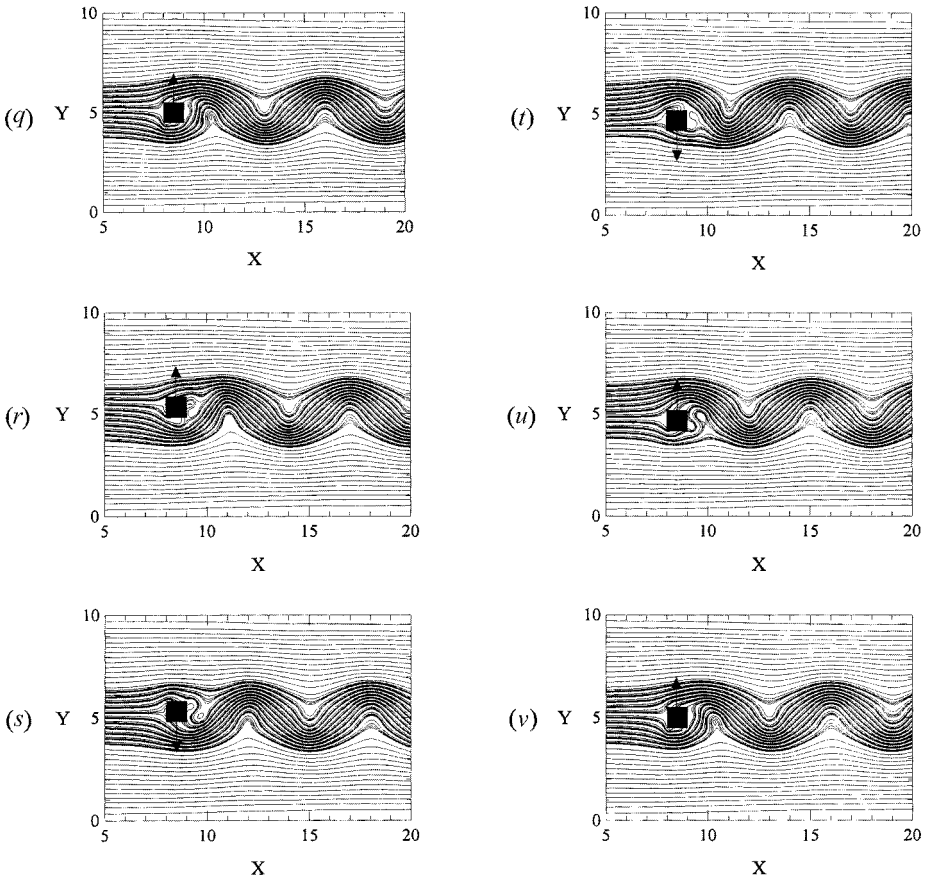

Figure 5. The transient developments of streamlines for case 1 (Re = 250, $S_c = 0.333$, $L_c = 0.5$, $\tau_p = 6.0$, $F_c = 0.167$, $B = 0.1$, $A = 1.0$). (*a*) $\tau = 0.5$, (*b*) $\tau = 1.5$, (*c*) $\tau = 2.0$, (*d*) $\tau = 3.0$, (*e*) $\tau = 4.0$, (*f*) $\tau = 4.5$, (*g*) $\tau = 5.0$, (*h*) $\tau = 6.0$, (*i*) $\tau = 7.0$, (*j*) $\tau = 8.0$, (*k*) $\tau = 10.0$, (*l*) $\tau = 12.0$, (*m*) $\tau = 15.0$, (*n*) $\tau = 18.0$, (*o*) $\tau = 33.0$, (*p*) $\tau = 36.0$, (*q*) $\tau = 42.0$, (*r*) $\tau = 43.0$, (*s*) $\tau = 44.0$, (*t*) $\tau = 46.0$, (*u*) $\tau = 47.0$, (*v*) $\tau = 48.0$

The rectangular cylinder turns downward immediately as it reaches the maximum upper amplitude. As shown in Figures 5*c*–5*d*, the rectangular cylinder is on the way to move downward. The fluid near the top surface of the rectangular cylinder simultaneously replenishes the vacant space induced by the movement of the rectangular cylinder. Consequently, a new recirculation zone is formed around the top surface of the rectangular cylinder. In the meantime, the fluid near the bottom surface of the rectangular cylinder is pressed by the bottom surface of the rectangular cylinder. As a result, the recirculation zone around the bottom surface of the rectangular cylinder is pressed by the bottom surface of the rectangular cylinder and then shed from the rectangular cylinder. Afterward, the new recirculation zone around the top surface of the rectangular cylinder enlarges gradually and pushes the vortex shedding away from the rectangular cylinder, as shown in Figures 5*e*–5*f*.

As the rectangular cylinder reaches the maximum downward amplitude, the rectangular cylinder returns upward immediately. As shown in Figures 5*g*–5*i*, the rectangular cylinder is on the way to move upward. The variations of the flow field around the rectangular cylinder are similar to the descriptions mentioned above.

Because of the vortex shedding and the oscillating motion of the rectangular cylinder, it is difficult for the large recirculation zones behind the rectangular cylinder to maintain their original situation. As a result, the large recirculation zones behind the rectangular cylinder split into small vortices and flow to the downstream, as shown in Figures 5*j*–5*l*.

As the time increases, because the rectangular cylinder is in oscillating motion, the recirculation zones are formed around the top and bottom surfaces of the rectangular cylinder alternatively and then shed from the rectangular cylinder, and flow to the downstream gradually. Because of the drastic swinging of the flow and the addition of vortices in the region behind the rectangular cylinder, the vortices are contracted and entrained in the flow gradually, and the flow becomes a wavy motion, as shown in Figures 5*m*–5*p*. The interaction between the oscillating rectangular cylinder and shedding vortex dominates the state of the wake.

Figures 5*q*–5*v* show the variations of the streamlines during one cycle of the oscillation motion as the flow field reaches a regular type. The streamlines at the time $\tau = 42.0$ (Figure 5*q*) are identical to those at the time $\tau = 48.0$ (Figure 5*v*), which means that the variations of the flow field become a periodic motion with time. As the variations of the flow patterns become a periodic state, the Strouhal number, St, is equal to 0.167, which is identical to the oscillation frequency of the rectangular cylinder. These phenomena are similar to entrainment processes [28] and the flow field is in a lock-in state.

Figure 6 shows the time history of the velocity V at the position of $X = 10.0$ and Y at the center of the rectangular cylinder for case 1. After the time $\tau > 30.0$, the variations of the velocity V become a periodic function of time and the Strouhal number is about 0.167, which is consistent with that mentioned above. The results show that the vortex shedding frequency gradually changes to match the oscillation frequency of the rectangular cylinder.

Figure 7 shows the transient developments of the isothermal lines for case 1. The variations of the thermal field usually correspond to the variations of the flow field. In Figures 7*a*–7*b*, the rectangular cylinder moves upward. Since the top surface of the rectangular cylinder presses the fluid near the top surface of the rectangular cylinder, the isothermal lines near the top surface of the rectangular cylinder become dense gradually, and the heat transfer is enhanced on the top surface of the rectangular cylinder. Conversely, because of the movement of the rectangular cylinder, the recirculation zone, which is disadvantageous to the heat transfer, is observed around the bottom surface of the rectangular cylinder. Thus, the isothermal lines near the bottom surface of the rectangular cylinder become sparse and extend to the neighborhood.

As shown in Figures 7*c*–7*f*, the rectangular cylinder is on the way to move downward. As mentioned above, the variations of the flow field are opposite to the rectangular cylinder moving upward. Thus, the isothermal lines gradually become dense near the bottom surface of the rectangular cylinder and sparse near

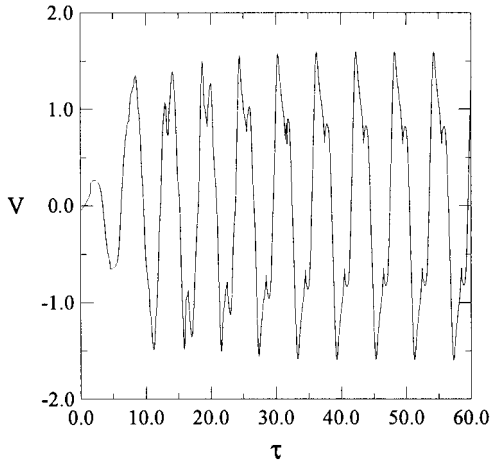

Figure 6. History of velocity V behind the rectangular cylinder as function of time for case 1 ($\mathrm{Re} = 250$, $S_c = 0.333$, $L_c = 0.5$, $\tau_p = 6.0$, $F_c = 0.167$, $B = 0.1$, $A = 1.0$).

the top surface of the rectangular cylinder. As for the front and rear surfaces of the rectangular cylinder, the variations of the isothermal lines near the front surface are slight; but the isothermal lines near the rear surface become denser gradually during the transient developments. In Figures 7*g*–7*h*, the rectangular cylinder is on the way to move upward. The variations of the thermal field are similar to the descriptions mentioned earlier.

Because the rectangular cylinder is in oscillating motion, the recirculation zones are formed around the top and bottom surfaces of the rectangular cylinder alternatively. Figures 7*i*-7*n* show the variations of the isothermal lines during one cycle of the oscillation motion as the flow field becomes a periodic state. The isothermal lines at the time (Figure 7*i*) are identical to those at the time $\tau = 48.0$ (Figure 7*n*), which means the variations of the thermal field become a periodic state with time as well as the flow field. Furthermore, the distributions of the isothermal lines around the rectangular cylinder are denser than those of the steady state (Figure 4*b*), which implies that the heat transfer around the rectangular cylinder is enhanced.

The variations of the average Nusselt numbers $\overline{\mathrm{Nu}}_X$ and $\overline{\mathrm{Nu}}_Y$ on each surface of the rectangular cylinder with time for case 1 are shown in Figure 8. Based upon these reasons mentioned above, the variations of the average Nusselt numbers would approach a periodic state. The enhancement of heat transfer on the top and bottom surfaces is remarkable and is slight on the front surface.

The variations of the overall Nusselt number Nu around the rectangular cylinder with time for case 1 are indicated in Figure 9*a*. In comparison with the heat transfer of the stationary rectangular cylinder ($\mathrm{Nu} = 5.44$), the heat transfer is enhanced about 35% for this case.

Figure 9*b* shows the variations of the overall Nusselt number Nu around the rectangular cylinder with time for case 2 ($\mathrm{Re} = 500$, $S_c = 0.333$, $\tau_p = 6.0$, $F_c = 0.167$, $L_c = 0.5$, $B = 0.1$, and $A = 1.0$). Basically, the variations of the flow

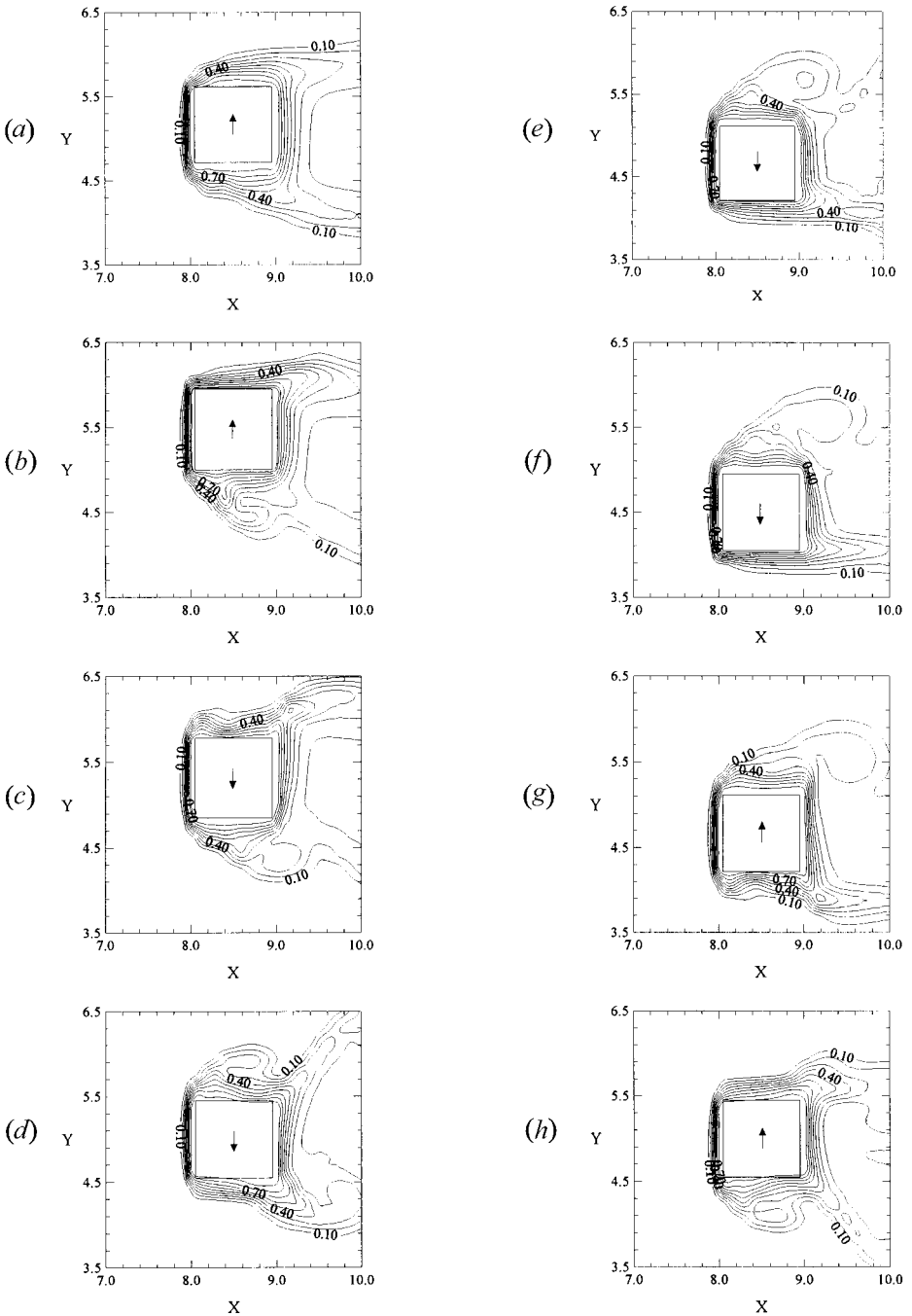

FIGURE 7

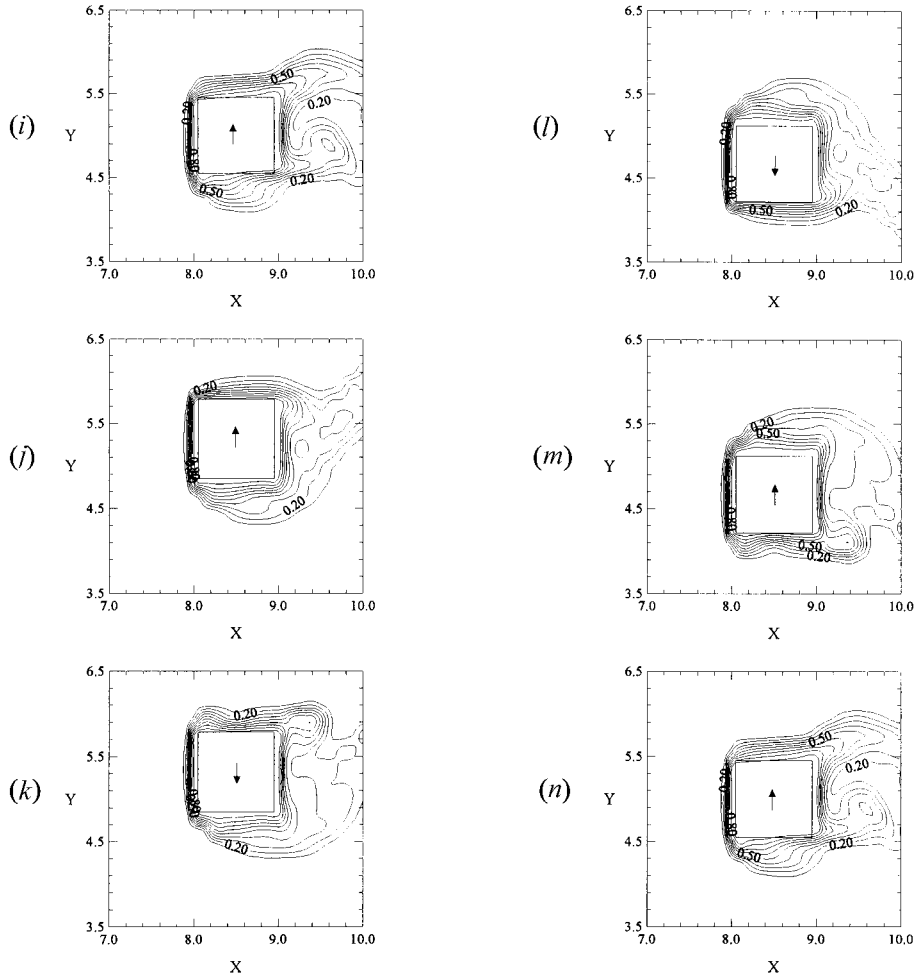

Figure 7. The transient developments of isothermal lines for case 1 ($\mathrm{Re} = 250$, $S_c = 0.333$, $L_c = 0.5$, $\tau_p = 6.0$, $F_c = 0.167$, $B = 0.1$, $A = 1.0$). (*a*) $\tau = 0.5$, (*b*) $\tau = 1.5$, (*c*) $\tau = 2.0$, (*d*) $\tau = 3.0$, (*e*) $\tau = 4.0$, (*f*) $\tau = 4.5$, (*g*) $\tau = 5.0$, (*h*) $\tau = 6.0$, (*i*) $\tau = 42.0$, (*j*) $\tau = 43.0$, (*k*) $\tau = 44.0$, (*l*) $\tau = 46.0$, (*m*) $\tau = 47.0$, (*n*) $\tau = 48.0$.

and thermal fields for this case are similar to the above case. Because of entrainment processes, the vortex shedding frequency is synchronized with the oscillation frequency of the rectangular cylinder. Consequently, the variations of flow patterns and thermal field become a periodic motion with time. In the computing region, the heat transfer around the oscillating rectangular cylinder is increased about 45% than that of a stationary rectangular cylinder under $\mathrm{Re} = 500$, $B = 0.1$, and $A = 1.0$ situation ($\mathrm{Nu} = 7.72$). In a comparison of the variations of the overall Nusselt number between case 1 and case 2, we see the enhancement of heat transfer increases with the increment of Reynolds number.

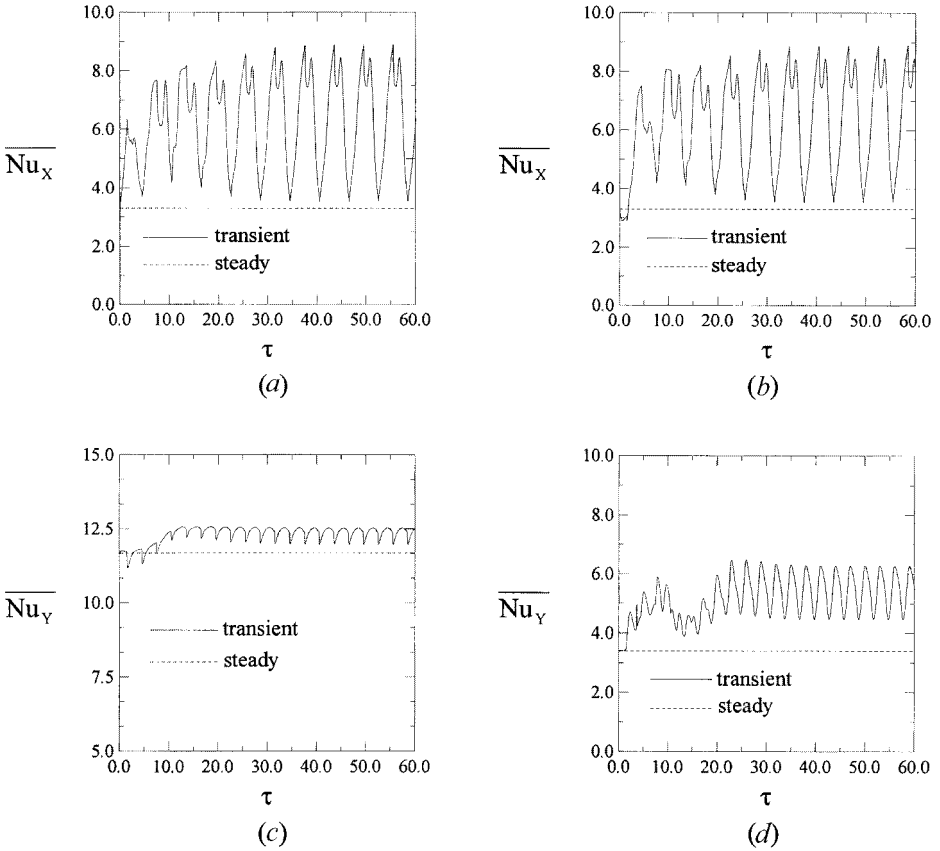

Figure 8. The variations of the average Nusselt number on the surfaces of the rectangular cylinder with time for case 1 ($\mathrm{Re} = 250$, $S_c = 0.333$, $\tau_p = 6.0$, $F_c = 0.167$, $L_c = 0.5$, $B = 0.1$, $A = 1.0$). (*a*) Top surface, (*b*) bottom surface, (*c*) front surface, (*d*) rear surface.

Effects of the Oscillating Amplitude on the Heat Transfer

Figure 10 shows variations of the overall Nusselt number Nu around the rectangular cylinder with time for various oscillating amplitudes under $\mathrm{Re} = 250$, $S_c = 0.5$, $B = 0.1$, and $A = 1.0$ situations. The heat transfer rates around the rectangular cylinder are increased about 13%, 40%, 54%, and 55% for the oscillating amplitude $L_c = 0.125$ (case 3), $L_c = 0.25$ (case 4), $L_c = 0.5$ (case 5), and $L_c = 0.75$ (case 6), respectively. As the oscillating amplitude of the rectangular cylinder is increased, the flow is disturbed more drastically and the heat transfer is enhanced more remarkably, which is consistent with the literature [6–9] for a circular cylinder oscillating in a flow.

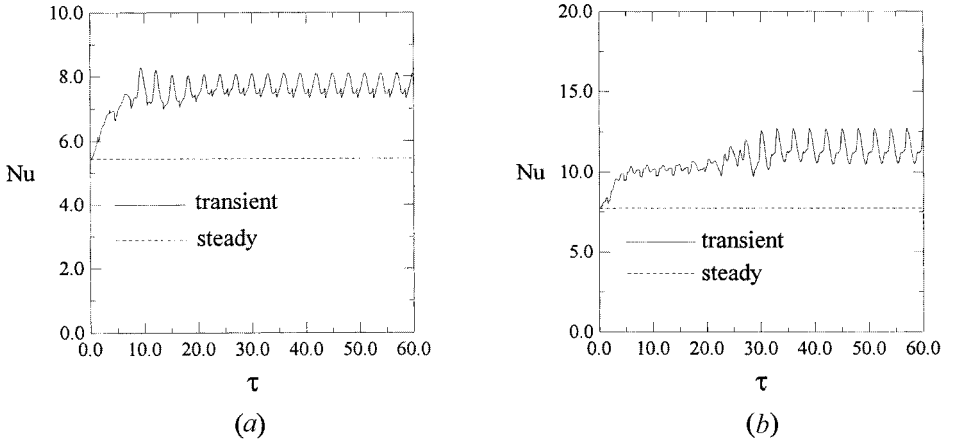

Figure 9. The variations of the overall Nusselt number around the surfaces of the rectangular cylinder with time. (*a*) Case 1 ($\mathrm{Re} = 250$, $S_c = 0.333$, $\tau_p = 6.0$, $F_c = 0.167$, $L_c = 0.5$, $B = 0.1$, $A = 1.0$), (*b*) case 2 ($\mathrm{Re} = 500$, $S_c = 0.333$, $\tau_p = 6.0$, $F_c = 0.167$, $L_c = 0.5$, $B = 0.1$, $A = 1.0$).

Effects of the Oscillating Speed on the Heat Transfer

The effects of the oscillating speed of the rectangular cylinder on the heat transfer are shown in Figures 9*b* and 11 for $\mathrm{Re} = 500$, $L_c = 0.5$, $B = 0.1$, and $A = 1.0$. The heat transfer rates around the rectangular cylinder are increased about 45%, 62%, and 115% for the oscillating speed $S_c = 0.333$ (case 2), $S_c = 0.5$ (case 7), and $S_c = 1.0$ (case 8), respectively. As the oscillating speed of the rectangular cylinder is increased, the variations of the flow become more drastic. Consequently, the heat transfer rate is enhanced remarkably with the increment of the oscillating speed.

Effects of the Blockage Ratio on the Heat Transfer

Figure 12*a* indicates the variations of the overall Nusselt number Nu around the rectangular cylinder with time for case 9 ($\mathrm{Re} = 500$, $S_c = 0.333$, $L_c = 0.5$, $\tau_p = 6.0$, $F_c = 0.167$, $B = 0.2$, and $A = 1.0$). In this case, the blockage ratio B is equal to 0.2, which means that the height of the channel is lower than that of case 2 ($B = 0.1$), and the flow velocity is increased. The variations of the flow and thermal fields for this case are similar to those of case 2. Comparing the variations of the overall Nusselt number of case 2 and case 9, the increment of the blockage ratio causes the flow and thermal fields to more rapidly reach a periodic state. In the computing region, the heat transfer around the rectangular cylinder is increased by about 38% than that of a stationary rectangular cylinder under $\mathrm{Re} = 500$, $B = 0.2$, and $A = 1.0$ situation ($\mathrm{Nu} = 8.7$)

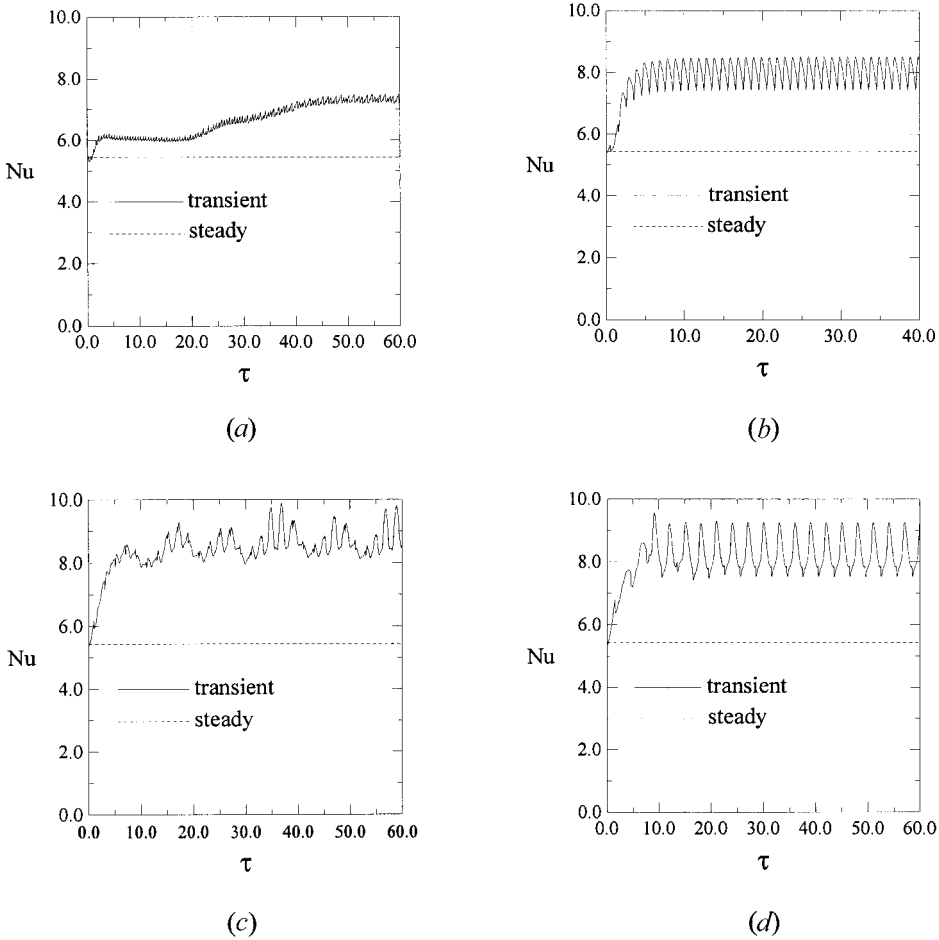

Figure 10. The variations of the overall Nusselt number around the surfaces of the rectangular cylinder with time for various oscillating amplitudes under $\mathrm{Re} = 250$, $S_c = 0.5$, $B = 0.1$, $A = 1.0$ situation. (*a*) Case 3: $L_c = 0.125$, $\tau_p = 1.0$, $F_c = 1.0$; (*b*) case 4: $L_c = 0.25$, $\tau_p = 2.0$, $F_c = 0.5$; (*c*) case 5: $L_c = 0.5$, $\tau_p = 4.0$, $F_c = 0.25$; (*d*) case 6: $L_c = 0.75$, $\tau_p = 6.0$, $F_c = 0.167$.

Effects of the Aspect Ratio on the Heat Transfer

The variations of the overall Nusselt number Nu around the rectangular cylinder with time for case 10 ($\mathrm{Re} = 500$, $S_c = 0.333$, $L_c = 0.5$, $\tau_p = 6.0$, $F_c = 0.167$, $B = 0.1$, and $A = 2.0$) are shown in Figure 12*b*. In this case, the aspect ratio A is equal to 2.0 and the heat transfer area of the top and bottom surface of the rectangular cylinder is larger than that of case 2 ($A = 1.0$). The heat transfer around the oscillating rectangular cylinder is increased by about 60% more than that of a stationary rectangular cylinder under $\mathrm{Re} = 500$, $B = 0.1$, and $A = 2.0$ situation ($\mathrm{Nu} = 4.7$). As mentioned above, because the enhancement of heat transfer is

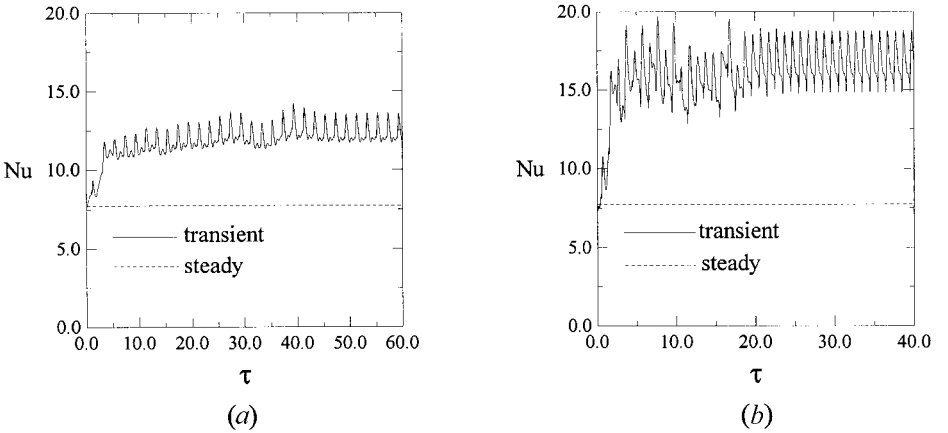

Figure 11. The variations of the overall Nusselt number around the surfaces of the rectangular cylinder with time for varoius oscillating speeds under $\mathrm{Re} = 500$, $L_c = 0.5$, $B = 0.1$, $A = 1.0$ situation. (*a*) Case 7: $S_c = 0.5$, $\tau_p = 4.0$, $F_c = 0.25$; (*b*) case 8: $S_c = 1.0$, $\tau_p = 2.0$, $F_c = 0.5$.

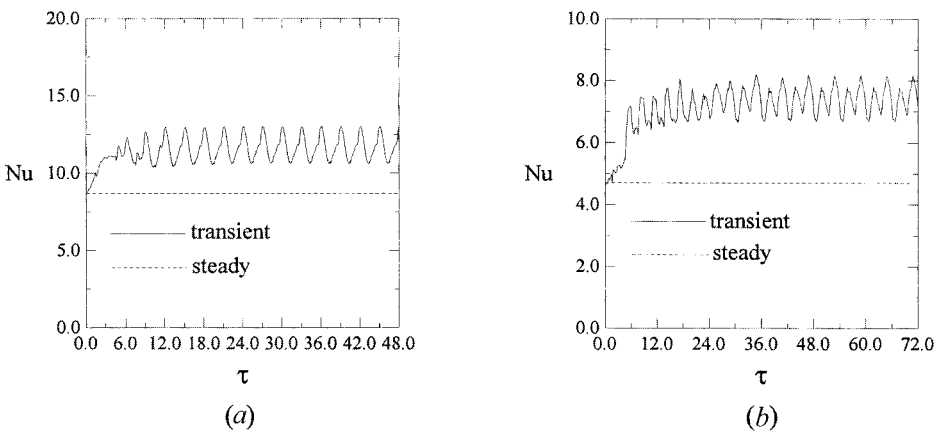

Figure 12. The variations of the overall Nusselt number around the surfaces of the rectangular cylinder with time. (*a*) Case 9 ($\mathrm{Re} = 500$, $S_c = 0.333$, $L_c = 0.5$, $\tau_p = 6.0$, $F_c = 0.167$, $B = 0.2$, $A = 1.0$), (*b*) case 10 ($\mathrm{Re} = 500$, $S_c = 0.333$, $L_c = 0.5$, $\tau_p = 6.0$, $F_c = 0.167$, $B = 0.1$, $A = 2.0$).

remarkable on the top and bottom surfaces of the rectangular cylinder, the heat transfer rate for this case is larger than that of case 2.

CONCLUSIONS

Numerical simulation is performed to study flow structures and heat transfer characteristics of a heated transversely oscillating rectangular cylinder in a cross flow. Some conclusions are summarized as follow.

1. The interaction between the oscillating rectangular cylinder and vortex shedding from the rectangular cylinder dominates the state of the wake. Because of the entrainment process, the vortex shedding frequency is changed to match the rectangular cylinder oscillation frequency gradually. The flow and thermal fields would approach a periodic state with time.
2. The heat transfer rates are enhanced remarkably as the oscillating amplitude and speed of the rectangular cylinder are increased.
3. Increasing the blockage ratio results in the flow and thermal fields more rapidly reaching a periodic state, and the heat transfer is also enhanced.
4. Increasing the aspect ratio causes the enhancement of the heat transfer to be increased.

REFERENCES

1. J. D. Hudson, S. C. R. Dennis, and N. Smith, Steady Laminar Forced Convection from a Circular Cylinder at Low Reynolds Numbers, *Physics of Fluids*, vol. 11, pp. 933–939, 1968.
2. P. C. Jain and B. S. Goel, A Numerical Study of Unsteady Laminar Forced Convection from a Circular Cylinder, *Journal of Heat Transfer*, vol. 98, pp. 303–307, 1976.
3. H. M. Badr, A Theoretical Study of Laminar Mixed Convection from a Horizontal Cylinder in a Cross Stream, *International Journal of Heat and Mass Transfer*, vol. 26, pp. 639–653, 1983.
4. G. E. Karniadakis, Numerical Simulation of Forced Convective Heat Transfer from a Cylinder in Crossflow, *International Journal of Heat and Mass Transfer*, vol. 31, pp. 107–118, 1988.
5. K. Sreenivasan and A. Ramachandran, Effect of Vibration of Heat Transfer from a Horizontal Cylinder to a Normal Air Stream, International *Journal of Heat and Mass Transfer*, vol. 3, pp. 60–67, 1961.
6. U. C. Saxena and A. D. K. Laird, Heat Transfer from a Cylinder Oscillating in a Cross-Flow, *Journal of Heat Transfer*, vol. 100, pp. 684–689, 1978.
7. C. T. Leung, N. W. M. Ko, and K. H. Ma, Heat Transfer from a Vibrating Cylinder, *Journal of Sound and Vibration*, vol. 75, pp. 581–582, 1981.
8. D. Karanth, G. W. Rankin, and K. Sridhar, A Finite Difference Calculation of Forced Convective Heat Transfer from an Oscillating Cylinder, *International Journal of Heat and Mass Transfer*, vol. 37, pp. 1619–1630, 1994.
9. C. Gau, J. M. Wu, and C. L. Liang, Heat Transfer Enhancement and Vortex Flow Structure over a Heated Cylinder Oscillating in the Crossflow Direction, *Journal of Heat Transfer*, vol. 121, pp. 789–795, 1999.
10. C. H. Cheng, H. N. Chen, and W. Aung, Experimental Study of the Effect of Transverse Oscillation on Convection Heat Transfer from a Circular Cylinder, *Journal of Heat Transfer, vol. 119, pp. 474–482, 1997.*
11. C. H. Cheng, J. L. Hong, and W. Aung, Numerical Prediction of Lock-on Effect on Convective Heat Transfer from a Transversely Oscillating Circular Cylinder, *International Journal of Heat and Mass Transfer*, vol. 40, pp. 1825–1834, 1997.
12. B. S. V. Patnaik, P. A. Aswatha, and K. N. Seetharamu, Numerical Simulation of Vortex Shedding Past a Circular under the Influence of Buoyancy, *International Journal of Heat and Mass Transfer*, vol. 42, pp. 3495–3507, 1999.
13. R. W. Davis and E. F. Moore, A Numerical Study of Vortex Shedding from Rectangles, *Journal of Fluid Mechanics*, vol. 116, pp. 475–506, 1982.

14. T. Igarashi, Heat Transfer from a Square Prism to an Air Stream, *International Journal of Heat and Mass Transfer*, vol. 28, pp. 175–181, 1985.
15. T. Igarashi, Local Heat Transfer from a Square Prism to an Air Stream, *International Journal of Heat and Mass Transfer*, vol. 29, pp. 777–784, 1986.
16. M. Yao, M. Nakatain, and K. Suzuki, Flow Visualization and Heat Transfer Experiments in a Turbulent Channel Flow Obstructed with an Inserted Square Rod, *International Journal of Heat and Fluid Flow*, vol. 16, pp. 389–397, 1995.
17 J. M. Chen and C. H. Liu, Vortex Shedding and Surface Pressures on a Square Cylinder at Incidence to a Uniform Air Stream, *International Journal of Heat and Fluid Flow*, vol. 20, pp. 592–597, 1999.
18. C. W. Hirt, A. A. Amsden, and H. K. Cooks, An Arbitrary Lagrangian-Eulerian Computing Method for All Flow Speeds, *Journal of Computational Physics*, vol. 14, pp. 227–253, 1974.
19. T. J. R. Hughes, W. K. Liu, and T. K. Zimmermann, Lagrangian–Eulerian Finite Element Formulation for Incompressible Viscous Flows, *Computer Methods in Applied Mechanics and Engineering*, vol. 29, pp. 329–349, 1981.
20. J. Donea, S. Giuliani, and J. P. Halleux, An Arbitrary Lagrangian-Eulerian Finite Element Method for Transient Dynamic Fluid-Structure Interactions, *Computer Methods in Applied Mechanics and Engineering*, vol. 33, pp. 689–723, 1982.
21. B. Ramaswamy and M. Kawahara, Arbitrary Lagrangian-Eulerian Finite Element Method for Unsteady, Convective, Incompressible Viscous Free Surface Fluid Flow, *International Journal for Numerical Methods in Fluids*, vol. 7, pp. 1053–1075, 1987.
22. B. Ramaswamy, Numerical Simulation of Unsteady Viscous Free Surface Flow, *Journal of Computational Physics*, vol. 90, pp. 396–430, 1990.
23. W. S. Fu and S. J. Yang, Numerical Simulation of Heat Transfer Induced by a Body Moving in the Same Direction as Flowing Fluids, *Heat and Mass Transfer*, vol. 36, pp. 257–264, 2000.
24. W. S. Fu and S. J. Yang, Heat Transfer Induced by a Body Moving in Opposition to a Flowing Fluid, *International Journal of Heat and Mass Transfer*, vol. 44, pp. 89–98, 2001.
25. W. S. Fu and S. J. Yang, A New Model for Heat Transfer of Fins Swinging Back and Forth in a Flow, *International Journal of Heat and Mass Transfer*, vol. 44, pp. 1687–1697, 2001.
26. J. N. Reddy and D. K. Gartling, The Finite Element Method in Heat Transfer and Fluid Dynamics, Chap. 4, CRC Press, Inc., Boca Raton, FL,1994.
27. W. S. Fu, T. M. Kau, and W. J. Shieh, Transient Laminar Natural Convection in an Enclosure from Steady Flow State to Stationary State, *Numerical Heat Transfer, Part A*, vol. 18, pp. 189–211, 1990.
28. H. M. Blackburn and R. D. Henderson, A Study of Two-dimensional Flow Past an Oscillating Cylinder, *Journal of Fluid Mechanics*, vol. 385, pp. 255–286, 1999.